Protein Science (1997), 6:569–579. Cambridge University Press. Printed in the USA.

Importance of the A-helix of the catalytic subunit of cAMP-dependent protein kinase for stability and for orienting subdomains at the cleft interface

FRIEDRICH W. HERBERG,[1] BASTIAN ZIMMERMANN,[1] MARIA McGLONE,[2] AND SUSAN S. TAYLOR[2]

[1]Institut für Physiologische Chemie, Abt. für Biochemie Supramolekularer Systeme, Ruhr-Universität Bochum, 44801 Bochum, Germany

[2]Department of Chemistry and Biochemistry, School of Medicine, University of California at San Diego, 9500 Gilman Drive, La Jolla, California 92093-0654

(RECEIVED October 10, 1996; ACCEPTED December 6, 1996)

Abstract

All eukaryotic protein kinases share a conserved catalytic core. In the catalytic (C) subunit of cAMP-dependent protein kinase (cAPK) this core is preceded by a myristylation motif followed by a long helix with Trp 30 at the end of this A-helix filling a hydrophobic cavity between the two lobes of the core. To understand the importance of the A-helix, the myristylation motif (Δ1–14) as well as the entire N-terminal segment (Δ1–39) were deleted. In addition, Trp 30 was replaced with both Tyr and Ala. All proteins were overexpressed in *E. coli* and purified to homogeneity. rC(Δ1–14), rC(W30Y), and rC(W30A) all had reduced thermostability, but were catalytically indistinguishable from wild-type C. Based on Surface Plasmon Resonance, all three also formed stable holoenzyme complexes with the RI-subunit, although the appKds were reduced by more than 10-fold due to decreases in the association rate. Surprisingly, however, the holoenzymes were even more thermostable than wild-type holoenzyme. To obtain active enzyme, it was necessary to purify rC(Δ1–39) as a fusion protein with glutathione-*S*-transferase (GST). GST-rC(Δ1–39), although its thermostability (T_m) was decreased by 12.5 °C, was catalytically similar to wild-type C and was inhibited by both the type I and II R-subunits and the heat-stable protein kinase inhibitor (PKI). The T_m for holoenzyme II formed with GST-rC(Δ1–39) was 16.5 °C greater than the T_m for free GST-rC(Δ1–39), and the K_a(cAMP) was increased nearly 10-fold. These mutants point out striking and unanticipated differences in how the RI and RII subunits associate with the C-subunit to form a stable holoenzyme and indicate, furthermore, that this N-terminal segment, far from the active site cleft, influences those interactions. The importance of the A-helix and Trp 30 for stability correlates with its location at the cleft interface where it orients the C-helix in the small lobe and the activation loop in the large lobe so that these subdomains are aligned in a way that allows for correct configuration of residues at the active site. This extensive network of contacts that links the A-helix directly to the active site in cAPK is compared to other kinases whose crystal structures have been solved.

Keywords: A-helix; cAPK; catalytic subunit; protein kinase

Reprint requests to: Susan S. Taylor, Department of Chemistry and Biochemistry, School of Medicine, 9500 Gilman Drive, University of California at San Diego, La Jolla, California 92093-0654; e-mail: staylor@ucsd.edu.

Abbreviations: AA, amino acid; ATP, adenosine triphosphate; BSA, bovine serum albumin; C, catalytic subunit of cAPK; cAMP, adenosine 3′,5′-cyclic monophosphate; cAPK, cAMP-dependent protein kinase; DTT, dithioerythreitol; EDC, *N*-ethyl-*N*′-(3-diethylaminopropyl)-carbodiimide; EGTA, [ethylenebis(oxyethylene-nitrilo)]tetraacetic acid; EDTA, *N,N,N′,N′*-ethylenediamine tetraacetic acid; GST, Glutathione-*S*-Transferase; IPTG, isopropyl-β-thiogalactopyranoside; MES, 2-(*N*-morpholino)ethanesulfonic acid; PMSF, phenylmethanesulfonyl fluoride; PKI, heat stable protein kinase inhibitor; MOPS, 3[*N*-morpholino]propane sulfonic acid; MW, molecular weight; NHS *N*-hydroxysuccinimide; R, regulatory subunit of cAPK; SDS, sodium dodecyl sulfate; SDS-PAGE, SDS polyacrylamide gel electrophoresis.

The conserved nature of the protein kinase catalytic core was first predicted when Barker and Dayhoff recognized sequence similarities between the gene product of the Rous Sarcoma Virus, $pp60^{v\text{-}src}$, and the catalytic (C) subunit of cAMP-dependent protein kinase-(cAPK) (Barker & Dayhoff, 1982). Hundreds of enzymes are now known to belong to this family, and all share the same general catalytic core (Hanks et al., 1988; Hanks & Hunter, 1995). The molecular features of this core were first defined when the structure of the catalytic subunit of cAPK was solved (Knighton et al., 1991). The catalytic core of this Ser/Thr kinase, defined as residues 42–297, consists of two lobes. The smaller amino terminal lobe constitutes the ATP binding domain, while the larger lobe contains most of the peptide binding sites and the residues respon-

sible for catalysis. Catalysis occurs at the cleft between the two lobes. Conserved residues within this core cluster largely around the active site cleft and contribute to ATP binding or catalysis (Taylor et al., 1993).

The subsequent solution of the crystal structures of cdk2 (De Bondt et al., 1993), MAP kinase (Zhang et al., 1994), the insulin receptor (Hubbard et al., 1994), phosphorylase kinase (Owen et al., 1995), twitchin kinase (Hu et al., 1994), and casein kinase I (Xu et al., 1995; Longenecker et al., 1996) confirmed the prediction that the general folding of the catalytic core would be conserved throughout the entire protein kinase family. From these structures we recognize not only the common features that are shared by all protein kinases but also the diversity of how these enzymes are regulated and how the conserved core interacts with the non-conserved regions that flank the core. The C-subunit core has an additional 39 residues at its amino N-terminus and an extra 50 residues at its carboxy C-terminus. The "extra" carboxy-terminal tail wraps around the surface of both lobes of the catalytic core with residues 301–318 anchored to the large lobe. The next segment, residues 319–346, is extended and spans the surface of both lobes, but the specific position it assumes relative to the core is dependent on whether the protein is in a "closed" or "open" conformation (Zheng et al., 1993; Chestukhin et al., 1996). The terminal four residues, including the terminal α-carboxylate, are buried in the small lobe.

The N-terminus is also anchored to both domains of the core, but, in contrast to the C-terminal tail, is not influenced significantly by opening and closing of the cleft. There are several well-defined components of this N-terminal docking motif. The N-terminus begins with a Gly that is myristylated (Carr et al., 1982). This acyl group folds into a well-defined acyl binding pocket (Zheng et al., 1993). Residues 1–14 encode the myristylation motif and constitute the first exon (Uhler et al., 1986). In the recombinant protein, which is not myristylated, this region is disordered. Residues 10–31 form a long amphipathic helix, the A-helix, that spans both lobes. The A-helix ends with Trp 30, which binds in a hydrophobic cavity that lies precisely between the two lobes on the surface that is opposite to the active site cleft. The extended segment from the helix to the beginning of the small lobe interacts with the surface of the small lobe.

The N-terminal docking motif and in particular the A-helix is strategically positioned, and an equivalent functional motif that complements the same surface of the core is probably a conserved feature of many protein kinases (Veron et al., 1993). The precise function of this motif, however, is unclear. To better understand the role that the A-helix, specifically, and the N-terminal docking motif, in general, play in the structure and function of the catalytic subunit, several mutations were introduced. Trp 30 was replaced with both Tyr and Ala, and two deletion mutants were constructed. The myristylation motif only (residues 1–14) was deleted, and the entire N-terminal segment, residues 1–39, were deleted. These mutant proteins, rC(W30Y), rC(W30A), rC(Δ1–14), and rC(Δ1–39) were purified to homogeneity and then characterized for catalytic activity, thermostability, and their ability to form complexes with three physiological inhibitors of C: the type I regulatory (RIα) subunit, the type II regulatory (RIIα) subunit, and the heat stable protein kinase inhibitor (PKI).

Results

Over-expression and purification of mutant proteins

All mutations were carried out as described in Experimental procedures. Expression and purification of the single site mutant proteins were essentially identical to the procedures that are used routinely for the wild type C-subunit. Both single site mutant proteins were mostly soluble when expressed at ≤30 °C. Typical yields were 10 mg/L of culture. Both point mutant proteins were purified first by P11 and then separated in three discrete isoforms by Mono S chromatography. The isoforms correspond to different phosphorylation states (Herberg et al., 1993). Isoform II was used for the biochemical analysis.

Unfortunately, expression of both deletion mutant proteins yielded completely insoluble protein under these conditions. Lysis in the presence of 1% Triton X-100 or 1 M NaCl, co-lysis with a mutant form of the RI-subunit, rR(R209K), or with PKI, and reduction of the temperature or the amount of IPTG added during protein expression all failed to give soluble protein. A new purification strategy was thus developed whereby mutant C-subunits (under ampicillin resistance) were co-expressed with GST-rR(Δ1-45:R209K) (under kanamycin resistance). This mutant R-subunit, fused to GST, has a reduced affinity for cAMP and binds the C-subunit very tightly (Bubis et al., 1988). Under these conditions, both rC(Δ1–14) and rC(Δ1–39) were found in the supernatant fraction in stoichiometric amounts relative to GST-rR(Δ1–45;R209K). A possible explanation is that the GST-rR(D1–45;R209K) works as a molecular chaperone by covering the hydrophobic surface of the D1–39 C-subunit, which, in contrast to the wild-type C-subunit, is exposed to solvent. The expression level of the GST-R was lower than the expression of the C-subunits, and the excess C-subunit was still insoluble. The presence of detergent (1% Triton X-100) during cell lysis was also essential to obtain soluble protein in this co-expression system. The soluble holoenzyme complex was then immobilized on glutathione agarose. rC(Δ1–14) was eluted by incubation with 100 μM cAMP. Typical yields were 1 mg of soluble C-subunit/L cell culture.

Surprisingly, however, and in contrast to rC(Δ1–14), rC(Δ1–39) could not be eluted from the agarose resin under similar conditions. Neither 10 mM cAMP, EDTA (10 mM), nor 1 M KCl were sufficient to elute rC(Δ1–39) based on activity assays and analytical gel filtration. A synthetic peptide corresponding to the A-helix, residues 15–39, in a 10-fold molar excess over the C-subunit, was also unable to compete the R-subunit away from the mutant C-subunit. As seen in Figure 1 (upper panel), when the holoenzyme complex was eluted from the agarose resin with glutathione, an equivalent amount of rC(Δ1–39) and GST-rR(Δ1–45;R209K) were released confirming that a complex had formed. The complex could not, however, be dissociated with cAMP. An alternative purification strategy was thus required (Fig. 1, lower panel).

Because the solubility of many proteins can be increased by expressing them as fusion proteins, a fusion protein with GST at the N-terminus of the rC(Δ1–39) mutation was constructed. At low temperature (22 °C) and with very low concentrations of IPTG (5 μM), this mutant protein expressed at satisfactory levels (Fig. 1, bottom panel) and yielded a partially (up to 70%) soluble, catalytically active protein that was inhibited stoichiometrically by PKI and the RI- and RII-subunits. GST-rC(Δ1–39) was immobilized on glutathione agarose and then eluted with glutathione. In addition, free rC(Δ1–39) was released by cleavage with thrombin.

Kinetic properties

To determine whether the kinetic properties of any of the mutant proteins were altered, the K_m values for ATP and peptide (Kemptide) were determined (Table 1). None of the mutant proteins showed

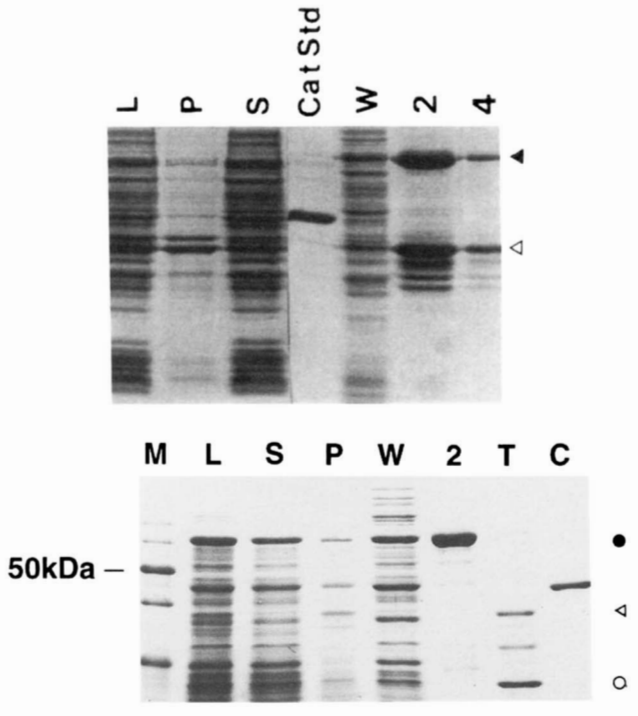

Fig. 1. Expression and purification of rC(Δ1–39). Upper panel: to obtain soluble enzyme rC(Δ1–39) was initially coexpressed with GST-rR(Δ1–45/R209K). The enzyme was soluble and was bound to glutathione agarose. Although cAMP failed to elute the C-subunit, elution with glutathione confirmed that equivalent amounts of GST-rR(Δ1–45/R209K) and rC(Δ1–39) were bound. The lanes are labeled as follows: L = total cell lysate; P = pellet; S = supernatant fractions following centrifugation of lysate; C, Cat std = C-subunit standard; W = buffer wash; 2,4 = fractions eluted from glutathione agarose with glutathione; the closed and open arrows correspond to = GST-rRI(Δ1–45/R209K) and = rC(Δ1–39), respectively. Lower panel: expression of rC(Δ1–39) as a GST-fusion protein. The lanes are labeled as indicated above. In addition, M = molecular weight markers; T = fractions after thrombin cleavage. The symbols are as follows: (open arrow), rC(Δ1–39); (closed circle), GST-rC(Δ1–39); (open circle), GST after cleavage.

any significant changes in the K_m values for MgATP and peptide substrate. Except for GST-rC(Δ1–39), the k_{cat} was also similar to the wild-type protein. Although the k_{cat} of GST-rC(Δ1–39) was reduced by 50%, this observed reduction is most likely attributed to the GST fusion itself because the wild-type C-subunit fused to GST showed a similar decrease in k_{cat} (S. Cox, pers. comm.). Because GST-rC(Δ1–39) lost activity quite rapidly, 30%/day at 4 °C, it was essential to assay the activity immediately following purification. Loss of activity for this mutant did not result in precipitation as was typical for the wild-type C-subunit, as demonstrated by analytical gel filtration. The inactive mutant fusion protein remained soluble.

Stokes radius

In contrast to the wild type-like kinetic properties of these mutated C-subunits, changes in some biophysical parameters were observed. All non-fused mutant proteins, for example, showed a small but significant increase in their Stokes' radius, indicating a change in the overall shape of the molecule (Table 1). The increase in R_s for rC(W30Y) and rC(W30A) was 1.3–1.5 Å compared to wild-type rC (R_s = 27.1 Å). Although rC(Δ1–14) did not show an increase in Stokes' radius in absolute numbers, a decrease had been expected because the molecular weight of the protein was reduced. The mammalian enzyme, myristylated at its N-terminus, and isoform III of the recombinant enzyme, which lacks a phosphate at Ser 10, both also show a decrease in the Stokes radius (R_s = 26.1–26.3 Å), confirming that the hydrodynamic properties of the protein are sensitive to perturbations in this region (Herberg et al., 1993).

Thermostability

The thermostability of these proteins was also characterized both in the presence and absence of R-subunit and MgATP. As summarized in Table 2, in comparison to the wild type rC-subunit, all of the free mutant C-subunits showed a decrease in thermostability (Fig. 2). GST-rC(Δ1–39) showed the strongest reduction in thermostability, displaying a T_m that was 12.5 °C lower than wild-type C-subunit. The stability of wild-type C-subunit is increased by divalent metals and ATP, and a similar increase of 5 °C was observed for rC(Δ1–39) in the presence of 1 mM ATP and 5 mM Mg.

Although the free mutant and deletion C-subunits were all less stable than the wild-type C-subunit, holoenzymes formed with these mutant C-subunits and the RI-subunit in the presence of MgATP were very stable. In fact, holoenzymes formed with rC(W30Y), rC(W30A), and rC(Δ1–14) were slightly more stable than the wild-type holoenzyme (Fig. 2; Table 2). The thermostability of GST-rC(Δ1–39) also increased when it was part of a

Table 1. *Biochemical characterization of A-helix mutant proteins*

		Point mutations		Deletion mutations	
	Wild-type	rC(W30A)	rC(W30Y)	rC(Δ1–14)	rC(Δ1–39)
Stokes' radius [Å]	27.1 ± 0.2	28.4	28.6	26.9	n.d.
k_{cat} [s^{-1}]	25[a]	20	24	25	10
K_m ATP [μM]	15	23	15	15	18
K_m peptide [μM]	23	26	30	23	29
PKI-Binding	Yes	Yes	Yes	Yes	Yes
K_a(cAMP) [nM] RI-holoenzyme	102 ± 9	157 ± 12	110 ± 10	140 ± 20	186 ± 23

[a]The k_{cat} of the wild-type GST-C-subunit was 12 s^{-1}. The Stoke's radius for the myristylated mammalian C-subunit was 26.1 Å (Herberg et al., 1993).

Table 2. *Thermal stability of the A-helix mutant proteins*[a]

		Point mutations		Deletion mutations	
	Wild-type	rC(W30A)	rC(W30Y)	rC(Δ1–14)	rC(Δ1–39)
Free C	46 ± 0.2	43.5 ± 0.2	43.0 ± 0.8	43.0 ± 1	33.5 ± 0.6
Free C +MgATP	51 ± 0.4	nd[b]	nd	48 ± 0.5	38.5 ± 0.5
ΔT_m (±ATPMg)	5	nd	nd	5	5
Type I holoenzyme	54.2 ± 0.2	56.4 ± 0.8	56.5 ± 0.4	56.2 ± 0.4	48 ± 2
ΔT_m (free C/holo)	8	12	12	12	15

[a]The T_ms were determined as described in Experimental procedures. The T_ms for the type I holoenzymes were determined in the presence of MgATP.
[b]nd = not determined.

holoenzyme complex; however, the stability varied significantly, depending on whether it was complexed with the RI or the RII subunit (Table 3). A major feature that distinguishes these two holoenzymes is their different requirement for MgATP. Unlike the type II holoenzyme, which does not require MgATP, stable type I holoenzyme does not form without MgATP (Herberg & Taylor, 1993). As seen in Figure 3, this difference in the MgATP dependency of the two holoenzymes is even more striking for GST-rC(Δ1–39). This mutant C-subunit also clearly shows that there are significant differences in how these two R-subunits interact with the C-subunit. Like free C and the other mutant C-subunits, the thermostability of free GST-rC(Δ1–39) and the corresponding type I holoenzyme was enhanced in the presence of MgATP. Most of the enhanced stability is due to the MgATP. Surprisingly, however, holoenzyme formed with GST-rC(Δ1–39) and the RII-subunit was just as stable as wild-type holoenzyme II. This is a difference of 16.5 °C and 18.5 °C between free C-subunit and the type II holoenzyme in the absence or presence of MgATP, respectively.

Characterization of holoenzymes

Based on these observations, two methods were used to further evaluate the stability of the mutant and wild type holoenzymes. Initially, the activation constants for cAMP were determined. In the presence of 1 mM DTT, the activation constants for holoenzymes formed with rC(W30A), rC(Δ1–14) and rC(Δ1–39) and the RI-subunit were slightly, but reproducibly, higher than wild-type and rC(W30A) holoenzymes (Fig. 4, Table 1). Surprisingly, the K_a(cAMP) for the type II holoenzyme formed with GST-rC(Δ1–39) was increased by nearly an order of magnitude. These higher K_a values were measured for both the phosphorylated and non-phosphorylated type II R-subunit (Table 3).

Surface plasmon resonance

Using Surface Plasmon Resonance (SPR), the association and dissociation rate constants were measured with wild-type and mutant C-subunits using rR(R209K), which was immobilized by amine

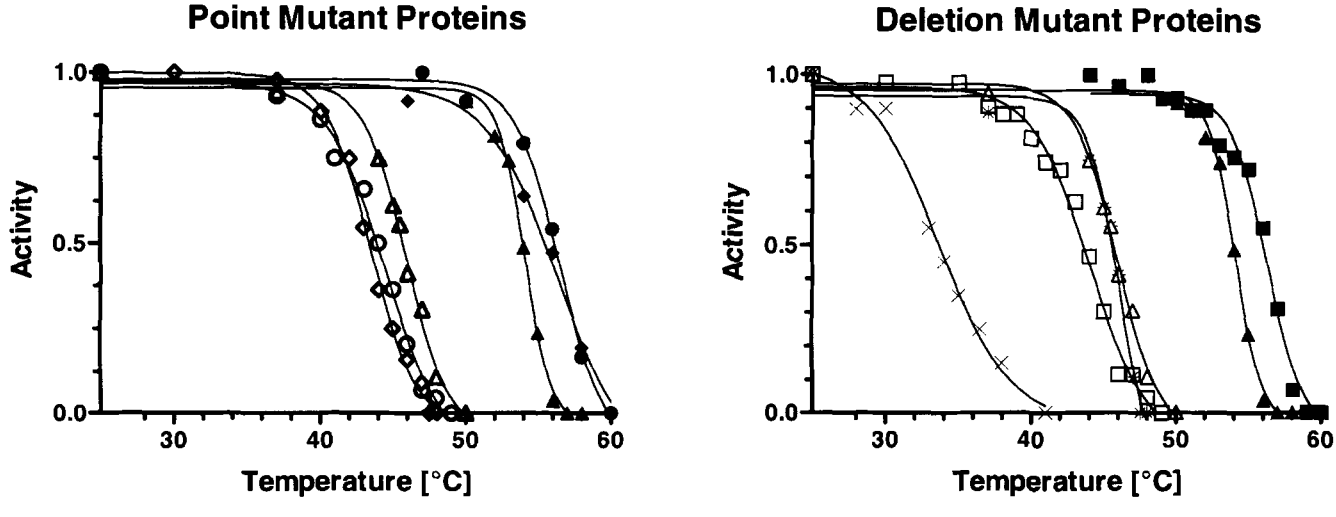

Fig. 2. Thermal inactivation of recombinant C-subunits. Thermal denaturation was carried out in 20 mM MOPS, 150 mM KCl, 1 mM DTT, pH 7.0 in the presence (closed symbols) or absence of type I R-subunit plus MgATP (open symbols). After incubating for two minutes at the temperatures indicated, the residual phosphotransfer activity was measured as described under Experimental procedures. Panel A shows the C-subunits having a single site mutation and wild-type C. Panel B shows C-subunits where the myristylation motif rC(Δ1–14) and the A-helix rC(Δ1–39) were deleted. For rC(Δ1–39) (×) corresponds to the free C-subunit and (*) to the type I holoenzyme. The C-subunits are indicated as follows: rC (open triangle, closed triangle); rC(W30A) (open diamond, closed diamond); rC(W30Y) (open circle, closed circle); rC(Δ1–14) (open square, closed square); rC(Δ1–39) (×, *).

Table 3. *Activation constants, K_a(cAMP), for holoenzymes formed with rC(Δ1–39) and wild-type C-subunits*

Holoenzyme	rC(Δ1–39) (nM)	WT (nM)
RI + MgATP	180	110
RII EDTA	850	105
RII + MgATP (P-RII)	1240	90

coupling to the surface of a sensor chip (Herberg et al., 1996). In contrast to the heat denaturation data reported above, SPR measures interaction between the two subunits of cAPK directly. These measurements were performed in the presence of 100 μM ATP and 1 mM $MgCl_2$. The rate constants are listed in Table 4, while the association and dissociation phases for rC(Δ1–39) and rR(R209K) are shown in Figure 5. Both rC(Δ1–14) and rC(W30A) showed a significantly reduced affinity for the RI-subunit. In both cases the kass was decreased 10-fold, indicating that the effect of these mutations was primarily on the initial interaction between the R- and C-subunits. The association rate constant for rC(W30Y) was more like wild-type C-subunit. The reduced affinity of rR(R209K) for these C-subunits that have mutations in the N-terminal docking region is in contrast to the K_as for cAMP, which indicated that the ability of cAMP to promote dissociation of the holoenzyme complexes is, if anything, impaired, particularly for the type II holoenzyme.

Discussion

In the C-subunit of cAPK the conserved catalytic core is preceded by a segment of 40 amino acids that is dominated by the A-helix, which makes many contacts with both lobes of the core. To elucidate the role of this helix for the function and structural stability of the C-subunit, several point and deletion mutations were introduced. Subsequent biochemical characterization of these mutant proteins focused on the role of the A-helix for activity, regulation, and thermostability. The results are correlated with the overall architecture of the enzyme and the interaction of the A-helix with different structural modules and subdomains within the C-subunit. The relationship of the A-helix to the kinase core in cAPK is then compared with other members of the protein kinase family, whose crystal structures are solved.

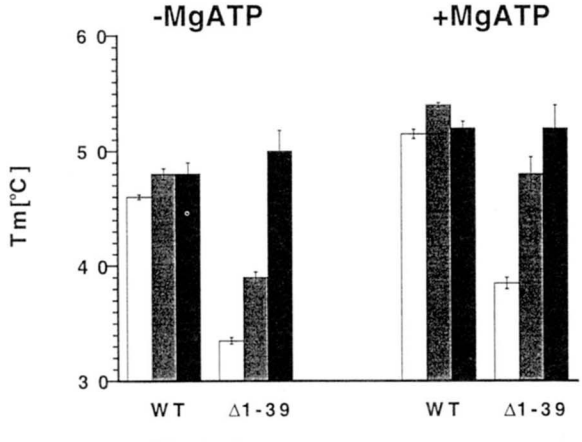

Fig. 3. Thermal stability (T_ms) of free rC(Δ1–39) and corresponding holoenzymes. The T_ms of free rC(Δ1–39) and the Type I and II holoenzymes are compared to the wild-type enzymes. T_ms were determined as described in Experimental procedures in the presence and absence of 1 mM ATP and 5 mM $MgCl_2$. White, gray, and black bars correspond to free C-subunit, type I holoenzyme, and type II holoenzyme.

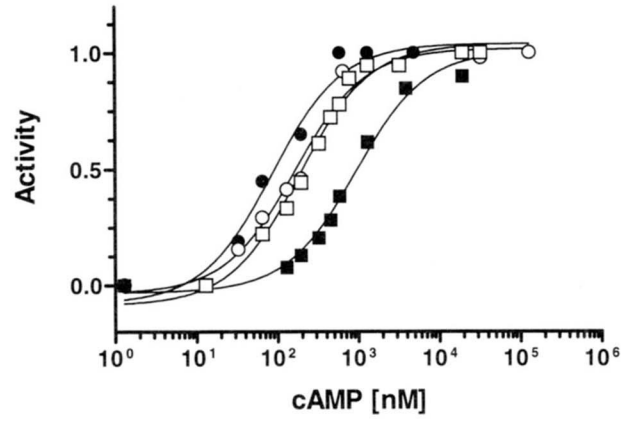

Fig. 4. Activation of holoenzymes by cAMP. The appKa for activation with cAMP were measured as described in Experimental procedures. Activation of the following holoenzymes are shown: wild-type C-subunit with wild-type rRIα (open circle); wild-type C-subunit with wild-type rRIIα (closed circle); rC(Δ1–39) with wild-type rRIα (open square); and rC(Δ1–39) with wild-type rRIIα (closed square).

The N-terminal segment of the C-subunit of cAPK, shown in Figure 6, is comprised of three distinct parts that each contribute to its docking to the surface of the kinase core. The myristylation motif is followed by a long amphipathic helix that spans the surface of both lobes. The most prominent feature of this helix is Trp 30, which binds in a deep hydrophobic cavity between the two lobes of the core (Fig. 6, right) (Veron et al., 1993). Trp 30 and Phe 26 fill this cavity and are specifically positioned between Arg 93 in the C-helix of the small lobe and Arg 190 in β strand 9 of the large lobe. The helix is followed by an extended strand that makes numerous contacts with the small lobe. The N-terminus thus shields an extended and mostly hydrophobic surface of the core.

Is the N-terminus important for catalytic activity or for stability and/or modulation of the core? Our results indicate that modification of the A-helix, including deletion of the entire helix, does not have a major effect on catalysis. When the protein was expressed as a soluble enzyme, the catalytic properties were similar to wild type C-subunit. The thermostability of the mutant proteins, however, was reduced significantly. Deletion of the myristylation motif was no worse than replacing Trp 30 with Ala, emphasizing the importance of filling this cavity. When the entire N-terminus was deleted, a "core" protein was generated that, with a T_m of 33 °C, would be inactive under physiological conditions. However, the in vitro catalytic properties of this "core" protein still resembled those of the wild type C-subunit, and the protein was still inhibited by PKI and the R-subunits. A major role of the A-helix in cAPK is thus to stabilize the core thermodynamically.

The proteins with deletions were particularly fragile and expression as a stable and soluble protein in *E. coli* required co-expression with the R-subunit or fusion to GST. GST-rC(Δ1–39) still lost activity quite rapidly, especially after removal of the GST segment. Providing the A-helix alone in a coexpression system with GST-

Table 4. *Surface plasmon resonance measurements of apparent binding constants for A-helix mutant proteins interacting with immobilized RI-subunit, rR(R209K)*

	WT	rC(W30A)	rC(W30Y)	rC(Δ1–14)	rC(Δ1–39)
$appk_{ass}$ (M^{-1} s^{-1})	3.5×10^6	0.49×10^6	4.04×10^6	0.42×10^6	0.55×10^6
$appk_{diss}$ (s^{-1})	2.4×10^{-4}	6.8×10^{-4}	8.2×10^{-4}	7.7×10^{-4}	2.1×10^{-4}
$appK_d$ (M)	0.07×10^{-9}	1.4×10^{-9}	0.2×10^{-9}	1.8×10^{-9}	0.4×10^{-9}

rC(1–39) and rC(Δ1–39) was not sufficient to stabilize or solubilize the mutant C-subunit (J. Lew, pers. comm.). Co-expression with an RI-subunit lacking cAMP binding domain B also did not yield soluble protein (data not shown), suggesting that some parts of the B-domain (Su et al., 1995), might be complementary to the A-helix in the deletion mutant.

The hydrodynamic properties of the C-subunit were also sensitive to perturbations in the N-terminus, as indicated by differences in the Stokes' radius. Both rC(W30A) and rC(W30Y) had a larger Stokes' radius by 1 Å than wild-type recombinant C-subunit (R_s = 27.1 Å) (Herberg et al., 1993). Compared to the myristylated mammalian enzyme (R_s = 26.1 Å) there is a 2 Å or 8% increase. This increase in Stokes' radius suggests that the A-helix might be loosely coupled to the core as a rigid body so that it can move away from the core or position itself somewhat differently when the invariant Trp 30 is mutated or the myristylation motif is removed (Fig. 6). The fact that the contacts between the N-terminus and the core are mostly hydrophobic could allow for this apparent loose coupling. This is also reflected in the higher thermal stability (T_m + 4C) for the myristylated rC-subunit in comparison to the unmyristylated rC-subunit (Yonemoto et al., 1993). The changes in stability and shape are consistent with the crystal structure of the myristylated C-subunit, where the N-terminus is most firmly anchored to the core in comparison to structures of the non-myristylated recombinant C-subunit. In this structure the myristic acid docks to a hydrophobic pocket on the surface of the large lobe (Zheng et al., 1993). In the structure of the unmyristylated rC-subunit where the acyl anchor is missing, the first 14 amino acids are not seen, suggesting that this segment is disordered (Knighton et al., 1991).

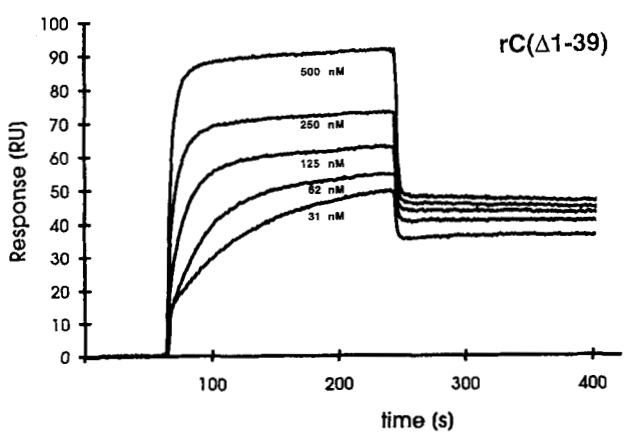

Fig. 5. Surface Plasmon Resonance measurements of rC(Δ1–39) with the RI-subunit, rR(R209K). Binding of rC(Δ1–39) to immobilized rR(R209K) was described in Experimental procedures. Measurements were taken over a concentration range from 31 to 500 nM rC(Δ1–39) as indicated.

Interfering with the acyl anchor either by removing the myristic acid or by deleting residues 1–14, introduces instability. Anchoring of the other end of the helix, specifically by Trp 30 filling a deep cavity, is weakened equivalently by the point mutations. These changes in stability that we observe with point mutations are consistent with other systems where altering a cavity introduces thermal instability (Eriksson et al., 1992).

The N-terminus also influences interaction with the R-subunits. For example, although the thermostability of the free C-subunit was decreased by all mutations, when the mutant C-subunits were complexed with the RI-subunit, the stability of the holoenzymes was equal to or greater than for the wild type protein. The ΔT_m (free C/holo) for the wild-type I holoenzyme was 8 °C higher than the subunit alone, in contrast to 12–15 °C for the mutant C-subunits (Table 2). These mutants not only demonstrated that the N-terminus influences how the R- and C-subunits associate with one another, but also show that there are significant differences between RI and RII. The difference was most apparent for rC(Δ1–39)/RII where the T_m for holoenzyme, although reduced by 12.5 °C to 33 °C for rC(Δ1–39) alone, was close to the value of the wild type holoenzyme (52 °C). Furthermore, and unlike the type I holoenzymes, the T_m for the type II holoenzyme was independent of MgATP. The activation constants, K_a(cAMP), for holoenzymes formed with rC(Δ1–39) further emphasize the differences between RI and RII. The K_a was increased nearly an order of magnitude for the type II holoenzyme in contrast to wild type-like K_as for the type I holoenzyme. The C-subunit thus interacts differently with the two R-subunits, with the N-terminus clearly being more important for interaction with the type II R-subunit.

Why is the N-terminal helix motif so important for the structural integrity of cAPK? The strategic position of Trp 30 relative to the core is seen in Figure 7. Although the A-helix itself is not conserved, it is juxtapositioned against motifs within the core that are highly conserved, and the orientation of these motifs or subdomains relative to one another at the cleft interface is critical for maintaining the active conformation of the enzyme (Fig. 7, left) (Johnson et al., 1996). In the small lobe, Arg 93 in the C-helix, which lines the top of the cavity filled by Trp 30, helps to position the C-helix so that Glu 91 can interact with Lys 72 in β strand 3. Trp 30 thus links the A-helix to the β sheet in the small lobe, and positions Lys 72 for its interactions with the α and β phosphates of ATP (Fig. 7, left). At the same time interactions with Arg 190 in β strand 9 of the large lobe stabilize the activation loop via interactions of Lys 189 and the essential phosphorylation site at Thr 197 (Fig. 7, right). The correct conformation of this activation loop is essential for catalysis (Adams et al., 1995).

The importance of the C-helix with its multiple interactions with various parts of the protein is apparent from Figure 8. In a single turn of this helix are Glu 91 pairing with Lys 72, Lys 92 pairing with the buried α-carboxylate of Phe 350, and Arg 93 interacting

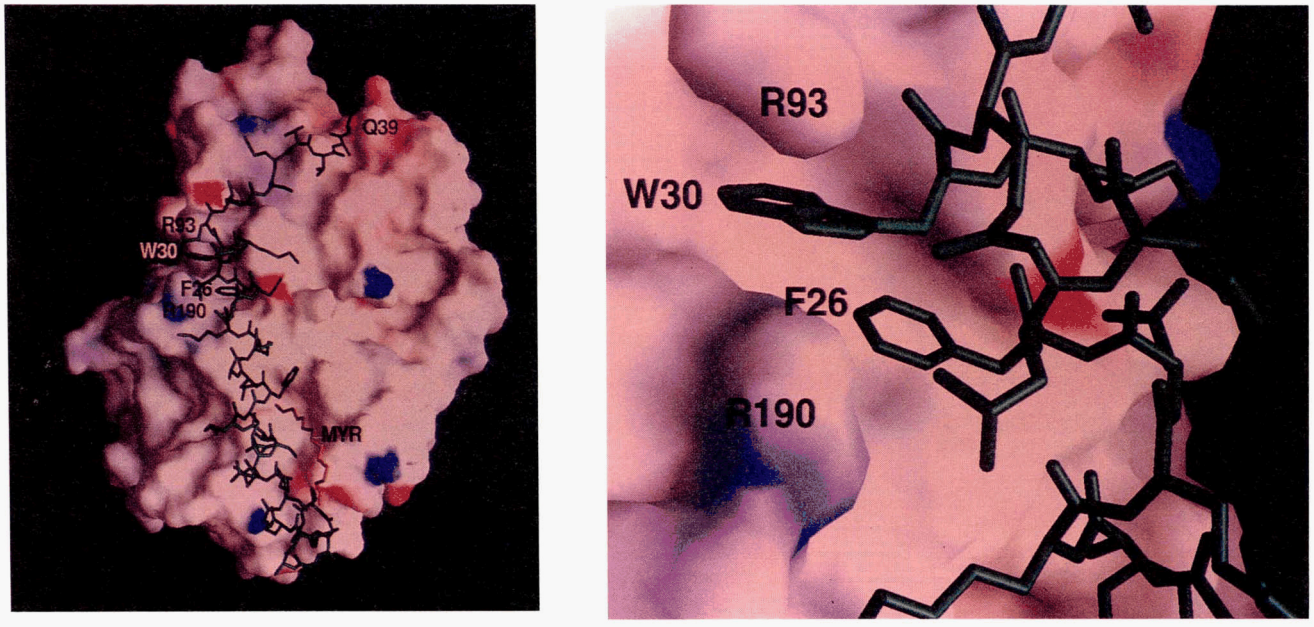

Fig. 6. Grasp model of the C-subunit of cAPK. On the left is the full-length C-subunit showing the extended surface of the A-helix that interacts with the core. The right panel shows the interactions of Trp 30 and Phe 26 of the A-helix with residues from the core. In this structure of the non-myristylated recombinant C-subunit the first 14 residues are disordered and not shown.

with Trp 30. One turn earlier is His 87 that pairs with the essential phosphorylation site, Thr 197, a conserved feature of the activation loop of many protein kinases (De Bondt et al., 1993; Hubbard et al., 1994; Zhang et al., 1994; Johnson et al., 1996). Lys 189, next to Arg 190, also binds this phosphate, as does Arg 165, which is adjacent to the proposed catalytic base, Asp 166 (Fig. 7, right). There is thus a well-defined network of interactions that extend in several directions from the A-helix to the active site, with the C-helix playing a central role in communicating between conserved and non-conserved subdomains (Veron et al., 1993).

As we acquire more structural information about different protein kinases, we can begin to appreciate the diversity of each kinase and hopefully discover some general rules. As a common feature, all protein kinases have a cavity between the two lobes whether it is a deep cavity as in cAPK and the γ-subunit of phosphorylase kinase (Owen et al., 1995) or a more shallow cavity as in cdk2 (De Bondt et al., 1993). The motif that complements this cavity, however, can differ. It is not necessary that the complementary motif be N-terminal to the core nor must it always be a helix.

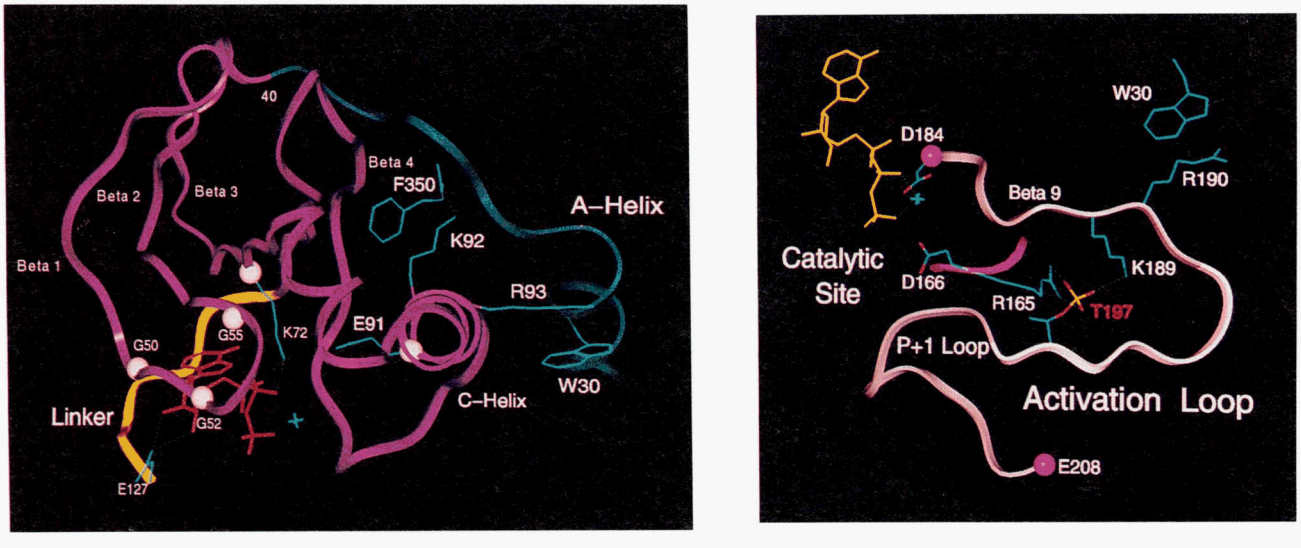

Fig. 7. A network of interactions link the A-helix to conserved motifs in both the small and large lobes of the kinase core. The left panel shows the network of interactions in the small lobe that link Trp 30 in the A helix to Lys 72 at the ATP binding site. The right panel shows a similar network of interactions that extend through β-strand 9 and the activation loop to the site of phosphoryl transfer.

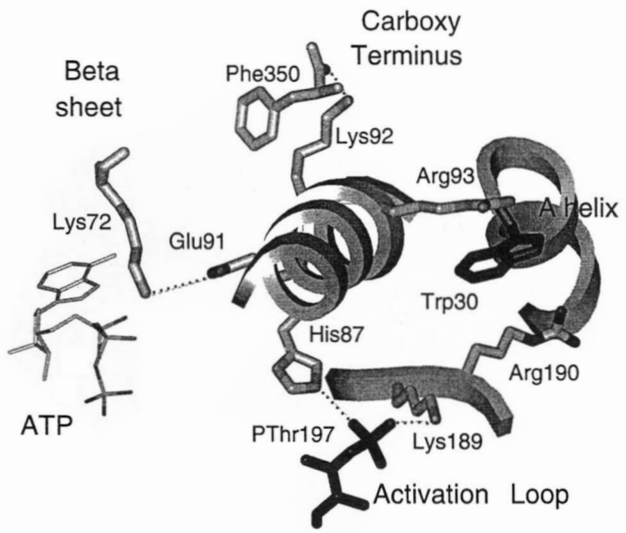

Fig. 8. Interactions of the C-helix with conserved and non-conserved regions of the catalytic subunit of cAPK. Residues in the C-helix make important contacts with many parts of the protein. Arg 93 and Lys 92 contact the A-helix and the C-terminus, respectively, both regions that are not conserved throughout the protein kinase family. Glu 91 and His 87, in contrast, bring together two critical conserved regions at the cleft interface.

Before considering some of these other structures, it is important to first recognize some differences between cAPK and the other kinase structures that have been solved to date. Unlike cAPK, most structures so far are not active enzymes. They lack the critical phosphate in the activation loop. Most other protein kinases are also not active physiologically as a small monomer. Many of the solved kinase structures are fragments that include little more than the kinase core. The structure of the C-subunit, in contrast, reflects a full length, fully active and correctly phosphorylated enzyme. Even the deletion mutant proteins are phosphorylated at Thr 197, because without this phosphate the enzyme has very altered kinetic properties (Adams et al., 1995). What does the structure of the complementary motif look like in other protein kinases?

In the case of the MAP kinase, the C-terminal tail folds over the large lobe and fills the same surface that is occupied in part by the A-helix in cAPK. Instead of a helix, an extended strand with two Phes, Phe 327 and Phe 329, filling the hydrophobic pocket, which in cAPK is filled by Trp 30 and Phe 26 (Zhang et al., 1994). This motif, positioned precisely between the conserved helix in the small lobe and β strand 9 and the activation loop in the large lobe, appears to fulfill the same function as the A-helix in cAPK. Phe 327 and Phe 329 in MAP kinase are thus structurally homologous to Trp 30 and Phe 26 and can be considered as an example of convergent evolution.

Phosphorylase kinase has no polypeptide chain covering the surface that includes the cavity (Owen et al., 1995), although two arginines equivalent to Arg 93 and Arg 190 in cAPK are in exactly the same position. Because the γ-subunit in phosphorylase kinase is part of a large hexadecameric complex, this surface is most likely filled by an adjacent subunit or by a portion of the C-terminus, which was deleted in the crystallized protein. In place of the phosphorylated Thr 197 there is a glutamate, which functionally mimics the phosphate, thus trapping the activation loop in a constitutively active conformation.

Like phosphorylase kinase, casein kinase I (CKI) also has no polypeptide covering the surface of the C-helix, which is masked by the A-helix in cAPK (Xu et al., 1995; Longenecker et al., 1996). These structures of yeast and mammalian enzymes represent active kinases but are missing 148 and 130 residues, respectively, at the C-terminus. This C-terminal tail contributes to membrane anchoring and/or autoregulation. Whether it folds over onto the C-helix in the full length protein, or whether or how this surface comes close to the membrane, is not known. The Arg in the C-helix corresponding to Arg 93 in cAPK is conserved as Arg or Lys in CKI, while the Arg corresponding to Arg 190 is replaced with Phe or Lys. Thus, a similar site is conserved.

Cdk2 alone does not have an equivalent to the A-helix either N- or C-terminal to the core, and the region corresponding to the C-helix and the activation loop of the core is disordered in the inactive and dephosphorylated enzyme (De Bondt et al., 1993; Taylor & Radzio-Andzelm, 1994; Radzio-Andzelm et al., 1995). Helix 3 in the small lobe (equivalent to the C-helix in cAPK) is twisted such that the conserved Glu, Glu 51, is facing the solvent rather than interacting with Lys 33. The activation loop is also ordered very differently. The equivalent of β-strand 9, for example, is completely missing. This disorder is largely corrected when cyclin binds (Jeffrey et al., 1995). Thus, in cdk2 it is cyclin, and not a contiguous A-helix, that correctly positions the C-helix and the activation loop at the cleft interface (Fig. 8).

In the truncated, inactive, and dephosphorylated insulin receptor, the helix in the small lobe is somewhat twisted and, like cdks, the activation loop again is ordered differently (Hubbard et al., 1994). The space that is filled by the N-terminal motif and by the activation loop in cAPK is empty in the insulin receptor. A major conformational change is thus required to assemble this part of the molecule into the conformation thought to be required to support catalysis. The N-terminal region of the insulin receptor is only partially present in this structure, and the Trp that was predicted to be analogous to Trp 30 in cAPK (Veron et al., 1993) is approaching this surface from a different direction. How this surface is complemented in the active enzyme has yet to be determined as well as what fills this surface in the inactive enzyme. It must be influenced in part by interactions of the protein with the membrane or with the complementary kinase domain of the dimer, and these interactions are presumably disrupted when insulin binds to the extracellular domain.

The importance of these non-core regions and the precise way in which they interact with and regulate the core has been demonstrated by Ahn et al., who analyzed the region of MAP kinase kinase (MAPKK) that immediately precedes the conserved core (Mansour et al., 1994; Engel et al., 1995). Replacing the essential phosphorylation sites in the activation loop with Glu generated an enzyme that was constitutively active in vitro, but this change alone was not sufficient to generate a constitutively active protein in vivo. However, after deletion of the segment that precedes the core, a region corresponding in sequence to the A-helix of cAPK, MAPKK was active both in vitro and in vivo. In MAP kinase activated protein kinase 2 (MAPKAP2), the C-terminus appears to function in a comparable way (Engel et al., 1995). The region that complements the cavity could thus have dual importance. It can stabilize an inactive conformation, as suggested in MAPKK, or it can stabilize an active conformation, as seen in cAPK. Obviously, the equilibrium between active and inactive conformations is a critical feature for all protein kinases. Clearly, many more structures are required before we can understand the full diversity of how the various kinases signal in this region of the molecule. The conformation of the inactive enzyme will not necessarily be con-

served; however, all protein kinases when fully active will assume a conformation at the cleft interface that resembles cAPK. Furthermore, it is already clear that this region is part of an extended network that can be extremely important for regulation even though the boundaries of this network lie a considerable distance from the site of phosphoryl transfer.

Experimental procedures

Reagents

The peptide substrate, LRRASLG, was synthesized using standard FMOC chemistry and purified by reverse phase HPLC (Kontron Instruments) or was purchased from Bachem Biochemicals. Other reagents were purchased as follows: ATP (Sigma), PMSF (Boehringer Mannheim), media supplies (Difco), phagemid $pRSET_B$ (Invitrogene), pUC4K (Pharmacia), restriction endonucleases and nucleic acid modifying enzymes (USB, Gibco/BLR and New England Biolabs). Materials used in cloning were molecular biology grade. The pGEX-KG vector was a gift from Dr. Jack Dixon (University of Michigan, Ann Arbor, MI).

Mutagenesis and expression

Mutagenesis was carried out by subcloning a 1.9 kbp NdeI/KpnI fragment of the catalytic subunit from pLWS-3 (Slice & Taylor, 1989) into the NdeI/KpnI sites of $pRSET_B$. Site-directed mutagenesis was performed with single stranded DNA according to Kunkel et al. (Kunkel et al., 1991) using the Muta-Gene Phagemid In Vitro Mutagenesis Kit (Biorad). All mutations were verified by dideoxy-DNA sequencing or by non-radioactive sequencing using an Applied Biosystems automated DNA sequencer.

The deletion mutants were constructed by engineering new NdeI sites at either residue 15 or residue 39. The Nde I generated fragment of either 52 bp or 120 bp was excised and the remaining $C\alpha/pRSET_B$ was religated and transformed into *E. coli* JM101.

The rC(Δ1–39) mutant was also subcloned into a GST-fusion vector. A synthetic linker in the GST fusion vector pGEX-KG (Guan & Dixon, 1991) was modified as described by Adams et al. (Adams et al., 1995) and the mutants were then subcloned into the NdeI/SstI sites of the pGEX-KG vector. Kanamycin resistance of pGEX-KG was accomplished by subcloning a pUC4K kanamycin gene into the Pst I site of pGEX-KG ampicillin gene. This abolished the ampicillin resistance of the GST fusion vector. Insertion and orientation were confirmed by DNA sequencing.

Mutagenesis of the RI(R209K)-subunit was accomplished by subcloning the 1.1 kbp Eco RI RI-subunit fragment into the Eco RI site of pUC118. Single-strand Kunkel DNA of this construct was prepared using the Muta-Gene Phagemid In Vitro Mutagenesis Kit. The RI(R209K)/pUC118 construct was digested with NcoI/HindIII. Due to an internal NcoI site, the resulting 0.95 kbp fragment lacked the first 45 amino acids of the regulatory subunit. This RI(Δ1–45/R209K) fragment was then subcloned into the NcoI/HindIII sites of a pGEX-KG vector (Guan & Dixon, 1991), which conveyed ampicillin resistance. Kanamycin resistance was achieved as described above.

Protein purification

The expression and purification of the rC(W30Y) and rC(W30A) mutants was similar to the procedures used for the wild-type C-subunit. Following overexpression in *E. coli* (Taylor et al., 1989) the cells were lysed in buffer A [30 mM MES, 1 mM EDTA, 50 mM KCl, 5 mM β-mercaptoethanol (βME), pH 6.5]. The C-subunits were purified by phosphocellulose chromatography (P11 Whatman) as described previously (Yonemoto et al., 1991) and were stored at 4 °C in buffer A or further purified using Mono S chromatography as described previously (Herberg et al., 1993). Typical yields were 10 mg/L of cell culture.

Both rC(Δ1–14) and the rC(Δ1–39) were purified as a holoenzyme following coexpression with GST-rR(R209K) as discussed above using the procedure of Smith and Johnson (Smith & Johnson, 1988). Six liters of cell pellets were resuspended in buffer B (20 mM potassium phosphate, 50 mM KCl, 5 mM EDTA, 5 mM DTT, 1% Triton X-100, pH 7.5) and lysed in a French Pressure cell (American Instrument). The crude lysate was then clarified for 45 min by centrifugation at 25,000 × *g* at 4 °C. The supernatant was batch bound for two hours at 4 °C to 12 mL of glutathione agarose, which was preswollen and equilibrated in buffer B. The resin was then transferred into a column (10 mm diameter) and washed three times with buffer B followed by two more washes of buffer B containing 250 mM KCl. The rC(Δ1–14) was eluted with 2–3 column volumes of buffer B containing 1 mM cAMP, 0.1% Triton X-100, and 50 mM KCl. The protein was then dialyzed against buffer C (20 mM MOPS, 150 mM KCl, 5 mM βME, pH 6.5) and stored at 4 °C. The GST-rC(Δ1–39) was eluted as a holoenzyme complex with 2 column volumes of 20 mM glutathione (Sigma) in buffer B, pH 7.5. Thrombin cleavage of the GST-fusion proteins was performed following the standard procedure for the GST-fusion kit (Guan & Dixon, 1991) (Pharmacia Biotech, procedure 12).

Recombinant RI-subunits were overexpressed in *E. coli* 222, purified as described previously (Saraswat et al., 1986), and stored at −20 °C in 20 mM potassium phosphate, 2 mM EDTA, 30% glycerol, 5 mM βME, pH 6.5 (buffer D). To obtain cAMP-free R-subunit, the R-subunit was unfolded with 8 M urea and refolded in buffer C as described by Buechler et al. (Buechler et al., 1993).

Protein purity was checked by SDS-polyacrylamide gel electrophoresis (Laemmli, 1970) and by analytical gel filtration.

Assays

The specific activity of the C-subunit was measured by a coupled spectrophotometric assay (Cook et al., 1982) using the heptapeptide, LRRASLG (Kemptide), as substrate. The standard assay was performed at 22 °C in buffer E (100 mM HEPES pH 7.0, 5 mM MgCl2, 1 mM ATP, 200 μM Kemptide).

Holoenzyme formation

Holoenzyme was formed by mixing C-subunit and cAMP-free (urea stripped) wild type RI-subunit in a 1:1 molar ratio in buffer C containing 100 μM ATP and 1 mM $MgCl_2$, pH 7.0.

Analytical gel filtration

Analytical gel filtration was carried out using a Superose 12 HR10/30 column or a Superdex 75 HR10/10 column both on a FPLC-system with a flow rate of 0.8 mL/min at 22 °C in buffer C as described previously (Herberg & Taylor, 1993).

K_a[cAMP]

Holoenzyme at a concentration of 30 nM C-subunit was incubated for 5 min at room temperature in buffer E with concentrations of

cAMP varying from 1 nM to 2.5 mM. The activity of the free C-subunit was then determined using the spectrophotometric assay.

Thermal denaturation

Heat denaturation was performed according to Yonemoto et al. (Yonemoto et al., 1993) using a spectrophotometric assay. C-subunits were diluted into buffer C to a final concentration of 0.1 mg/mL. This diluted enzyme (30 μL) was incubated for two minutes at various temperatures ranging from 22 °C to 60 °C. Aliquots of the heat-treated and untreated C-subunits were transferred into buffer E to a final concentration of 50 nM C-subunit. The percentage decrease in phosphotransferase activity was calculated by comparing the activity of the heat treated samples to the control samples using Prism software (Graphpad Inc., San Diego, CA). The apparent T_m corresponds to the temperature at which 50% residual activity remained after heat treatment. The analysis of the thermostability of the holoenzymes formed with the recombinant RI-subunit and the rC-subunit as described above was performed under the same conditions. The holoenzyme complex was activated by the addition of 10 μM cAMP.

Determination of protein concentration

Protein concentrations for C-subunit were determined spectrophotometrically at 280 nm using an extinction coefficient of $\epsilon_{\lambda 280} = 1.2 \times 10^3\ L \cdot M^{-1} \cdot cm^{-1}$ or according to Bradford (Bradford, 1976). In the presence of detergent the C-subunit was either titrated with a known amount of PKI or analyzed by SDS-PAGE using BSA as a standard and then scanning the protein bands with a Cybertech CS1 photo scanner.

Surface plasmon resonance

Surface Plasmon Resonance experiments were performed using a BIAcore instrument (Pharmacia/Biosensor). A mutant of the RI-subunit, RI(R209K), was prepared and immobilized as described previously (Herberg et al., 1994). This mutant R-subunit forms holoenzyme instantaneously and is dissociated by micromolar concentrations of cAMP (Herberg et al., 1996). To obtain association and dissociation rate constants and to calculate apparent KDs, the interactions between analyte and ligand were measured at concentrations between 25 and 500 nM protein in buffer C. In the association phase the interactions were monitored for 350 s. The dissociation phase was then monitored for one hour, with a concentration of 500 nM C-subunit.

Acknowledgments

This work was supported by Grants He1818-2/1 and SFB1524/B4 from the Deutsche Forschungsgemeinschaft (F.W.H. and B.Z.) and by Grant BE-48J from the American Cancer Society (S.S.T.). We thank Dr. Sarah Cox for the construction of the GST-Δ1–45:R209K-R-subunit and Mousoumi Majumdar, Marco DeStefano, Lily Huang, and Poopak Banky for technical support.

References

Adams JA, McGlone ML, Gibson R, Taylor SS. 1995. Phosphorylation modulates catalytic function and regulation in cAMP-dependent protein kinase. *Biochemistry 34*:2447–2454.

Barker WC, Dayhoff MO. 1982. Viral src gene products are related to the catalytic chain of mammalian cAMP-dependent protein kinase. *Proc Natl Acad Sci USA 79*:2836–2839.

Bradford MM. 1976. A rapid and sensitive method for the quantitation of microgram quantities of protein utilizing the principle of protein-dye binding. *Anal Biochem 72*:248–254.

Bubis J, Neitzel JJ, Saraswat LD, Taylor SS. 1988. A point mutation abolishes binding of cAMP to site A in the regulatory subunit of cAMP-dependent protein kinase. *J Biol Chem 263*:9668–9673.

Buechler YJ, Herberg FW, Taylor SS. 1993. Regulation defective mutants of type I cAMP-dependent protein kinase: Consequences of replacing Arg 94 and Arg 95. *J Biol Chem 268*:16495–16503.

Carr SA, Biemann K, Shoji S, Parmalee DC, Titani K. 1982. n-Tetradecanoyl in the NH_2 terminal blocking group of the catalytic subunit of the cyclic AMP-dependent protein kinase from bovine cardiac muscle. *Proc Natl Acad Sci USA 79*:6128–6131.

Chestukhin A, Litovchick L, Schourov D, Cox S, Taylor SS, Shalteil S. 1996. Functional malleability of the carboxy-terminal in protein kinase A. *J Biol Chem 271*:10175–10182.

Cook PF, Neville ME, Vrana KE, Hartl FT, Roskoski R. 1982. Adenosine cyclic 3′,5′-monophosphate dependent protein kinase: Kinetic mechanism for the bovine skeletal muscle catalytic subunit. *Biochemistry 21*:5794–5799.

De Bondt HL, Rosenblatt J, Jancarik J, Jones HD, Morgan DO, Kim SH. 1993. Crystal structure of cyclin-dependent kinase 2. *Nature 363*:595–602.

Engel K, Schultz H, Martin F, Kotlyarov A, Plath K, Hahn M, Heinemann U, Gaestel M. 1995. Constitutive activation of mitogen-activated protein kinase-activated protine kinase 2 by mutation of phosphorylation sites and an a-helix motif. *J Biol Chem 270*:27213–27221.

Eriksson AE, Baase WA, Zhang X-J, Heinz DW, Blaber M, Baldwin EP, Mathews BW. 1992. Response of a protein structure to cavity-creating mutations and its relation to the hydrophobic effect. *Science 255*:178–183.

Guan KL, Dixon JE. 1991. Eukaryotic proteins expressed in *Escherichia coli*: An improved thrombin cleavage and purification procedure of fusion proteins with glutathione *S*-transferase. *Anal Biochem 192*:262–267.

Hanks SK, Hunter T. 1995. Protein kinases 6. The eukaryotic protein kinase superfamily: Kinase (catalytic) domain structure and classification. *FASEB Jl 9*:576–596.

Hanks SK, Quinn AM, Hunter T. 1988. The protein kinase family: Conserved features and deduced phylogeny of the catalytic domains. *Science 241*: 42–52.

Herberg FW, Bell SM, Taylor SS. 1993. Expression of the catalytic subunit of cAMP-dependent protein kinase in *E. coli*: Multiple isozymes reflect different phosphorylation states. *Protein Eng 6*:771–777.

Herberg FW, Dostmann WRG, Zorn M, Davis SJ, Taylor SS. 1994. Crosstalk between domains in the regulatory subunit of cAMP-dependent protein kinase: Influence of amino terminus on cAMP binding and holoenzyme formation. *Biochemistry 33*:7485–7494.

Herberg FW, Taylor SS. 1993. Physiological inhibitors of the catalytic subunit of cAMP-dependent protein kinase: Effect of MgATP on protein/protein interaction. *Biochemistry 32*:14015–14022.

Herberg FW, Taylor SS, Dostman WRG. 1996. Active site mutations define the pathway for the cooperative activation of cAMP-dependent protein kinase. *Biochemistry 35*:2934–2942.

Hu S-H, Parker MW, Lei JY, Wilce MCJ, Benian GM, Kemp BE. 1994. Insights into autoregulation from the crystal structure of twitchin kinase. *Nature 369*:578–581.

Hubbard SR, Wei L, Ellis L, Hendrickson WA. 1994. Crystal structure of the tyrosine kinase domain of the human insulin receptor [see comments]. *Nature 372*:746–754.

Jeffrey PD, Russo AA, Polyak K, Gibbs E, Hurwitz J, Massague J, Pavletich NP. 1995. Mechanism of CDK activation revealed by the structure of a cyclin A-CDK2 complex. *Nature 376*:313–320.

Johnson LN, Noble ME, Owen DJ. 1996. Active and inactive protein kinases: Structural basis for regulation. *Cell 85*:149–158.

Knighton DR, Zheng J, Ten Eyck LF, Ashford VA, Xuong N-h, Taylor SS, Sowadski JM. 1991. Crystal structure of the catalytic subunit of cAMP-dependent protein kinase. *Science 253*:407–414.

Kunkel TA, Benebek K, McClary J. 1991. *Methods in Enzymology*. San Diego: Academic Press, Inc.

Laemmli UK. 1970. Cleavage of structural protein during the assembly of the head of bacteriophage T4. *Nature 227*:680–685.

Longenecker KL, Roach PJ, Hurley TD. 1996. Three-dimensional structure of mammalian casein kinase I: Molecular basis for phosphate recognition. *J Mol Biol 257*:618–631.

Mansour SJ, Matten WT, Hermann AS, Candia JM, Rong S, Fukasawa K, Woude GFV, Ahn NG. 1994. Transformation of mammalian cells by constitutively active MAP kinase kinase. *Science 265*:966–970.

Owen DJ, Noble ME, Garman EF, Papageorgiou AC, Johnson LN. 1995. Two structures of the catalytic domain of phosphorylase kinase: An active protein kinase complexed with substrate analogue and product. *Structure 3*:467–482.

Radzio-Andzelm E, Lew J, Taylor SS. 1995. Bound to activate: Conformational consequences of cyclin binding to CDK2. *Structure 3*:1135–1141.

Saraswat LD, Filutowics M, Taylor SS. 1986. Expression of the type I regulatory subunit of cAMP-dependent protein kinase in *Escherichia coli*. *J Biol Chem 261*:11091–11096.

Slice LW, Taylor SS. 1989. Expression of the catalytic subunit of cAMP-dependent protein kinase in *Escherichia coli*. *J Biol Chem 264*:20940–20946.

Smith DB, Johnson KS. 1988. Single-step purification of polypeptides expressed in *Escherichia coli* as fusions with glutathione *S*-transferase. *Gene 67*:31–40.

Su Y, Dostmann WRG, Herberg FW, Durick K, Xuong N-h, Ten Eyck L, Taylor SS, Varughese KI. 1995. Regulatory subunit of protein kinase A: Structure of deletion mutant with cAMP binding domains. *Science 269*:807–813.

Taylor SS, Buechler J, Slice L, Knighton D, Durgerian S, Ringheim G, Neitzel J, Yonemoto W, Dostmann W, Sowadski J. 1989. cAMP-dependent protein kinase: A framework for a diverse family of enzymes. *Cold Spring Harb Symp 53*:121–130.

Taylor SS, Knighton DR, Zheng J, Sowadski JM, Gibbs CS, Zoller MJ. 1993. A template for the protein kinase family. *Trends Biosci 18*:84–89.

Taylor SS, Radzio-Andzelm E. 1994. Three protein kinase structures define a common motif. *Structure 2*:345–355.

Uhler MD, Carmichael DF, Lee DC, Chivia JC, Krebs EG, McKnight GS. 1986. Isolation of cDNA clones for the catalytic subunit of mouse cAMP-dependent protein kinase. *Proc Natl Acad Sci USA 83*:1300–1304.

Veron M, Radzio-Andzelm E, Tsigelny I, Ten Eyck LF, Taylor SS. 1993. A conserved helix motif complements the protein kinase core. *Proc Nat Acad Sci USA 90*:10618–10622.

Xu R-M, Carmel G, Sweet RM, Kuret J, Cheng X. 1995. Crystal structure of casein kinase-1, a phosphate-directed protein kinase. *EMBO J 14*:1015–1023.

Yonemoto W, McGlone ML, Slice LW, Taylor SS. 1991. *Protein Phosphorylation (Part A)*. San Diego: Academic Press, Inc.

Yonemoto W, McGlone ML, Taylor SS. 1993. N-myristylation of the catalytic subunit of cAMP-dependent protein kinase conveys structural stability. *J Biol Chem 268*:2348–2352.

Zhang F, Strand A, Robbins D, Cobb MH, Goldsmith EJ. 1994. The crystal structures of ERK2 and a MgATP complex reveal the complex conformational restraints that appear to suppress kinase activity in the unphosphorylated enzyme. *Nature 367*:704–711.

Zheng J, Knighton DR, Xuong N-h, Taylor SS, Sowadski JM, Ten Eyck LF 1993. Crystal structures of the myristylated catalytic subunit of cAMP-dependent protein kinase reveal open and closed conformations. *Protein Sci 2*:1559–1573.